

The **next generation** GBCA
from Guerbet is here

Explore new possibilities >

Guerbet | 

© Guerbet 2024 GUOB220151-A

AJNR

This information is current as
of March 20, 2024.

MR High-Resolution Blood Oxygenation Level– Dependent Venography of Occult (Low-Flow) Vascular Lesions

Benjamin C.P. Lee, Katie D. Vo, Daniel K. Kido, Pratik
Mukherjee, Juergen Reichenbach, Weili Lin, Myeong S. Yoon and
Mark Haacke

AJNR Am J Neuroradiol 1999, 20 (7) 1239-1242
<http://www.ajnr.org/content/20/7/1239>

MR High-Resolution Blood Oxygenation Level–Dependent Venography of Occult (Low-Flow) Vascular Lesions

Benjamin C.P. Lee, Katie D. Vo, Daniel K. Kido, Pratik Mukherjee, Juergen Reichenbach, Weili Lin, Myeong S. Yoon, and Mark Haacke

Summary: A new technique for detecting vascular malformations, high-resolution BOLD venography (HRBV), is described. This technique relies on the BOLD principle for detecting deoxygenated blood in low-flow malformations. HRBV images are acquired using a modified 3D gradient-echo with voxel volumes of $0.5 \times 0.5 \times 2 \text{ mm}^3$. The magnitude data are masked with the phase images to enhance visibility of the venous structures and are displayed using the minimum intensity projection. Preliminary results for 10 patients show that HRBV is more sensitive in detecting cavernomas than is T2*-weighted imaging, and lesions that are presumed to be telangiectasias are detected only with this technique.

Low-flow vascular malformations are detected on MR images only after they have bled (1–6). The abnormal vessels of the malformations are shown unreliably with contrast enhancement and are rarely visible on conventional MR angiograms (7). A method of 3D gradient-echo MR venography, the high-resolution BOLD venography (HRBV) technique, which is capable of showing venous anatomy at submillimeter resolution, has been developed at our institution (8, 9). This technique is useful for characterizing these malformations and currently seems to be the only reliable method for detecting nonhemorrhagic cavernomas and telangiectasias.

Technique

HRBV was performed, without the intravenous administration of contrast material, as part of the clinical MR examinations. The HRBV images were acquired with a 3D fast low-angle shot sequence with a TE of 40, a low bandwidth (78 Hz/pixel), gradient moment nulling in all three orthogonal directions, 24 partitions, and a voxel volume of $0.5 \times 0.5 \times 2 \text{ mm}^3$. The total acquisition time was 8 minutes. In addition to standard T1-weighted and turbo T2-weighted images, gradient-echo echo-planar images (TE, 40; axial section, 5 mm; matrix, 128×128 interpolated to 256×256), 3D time-of-

flight MR angiograms (matrix, 512×512 ; section thickness, 1 mm), and 2D MR venograms (matrix, 256×256 ; section thickness, 2 mm) were obtained. Using a conventional circularly polarized (CP) head coil, all imaging was conducted on a 1.5-T Vision system (Siemens, Erlangen, Germany).

To enhance the visibility of the venous structures, the magnitude images were manipulated with the phase data by the use of the “phase mask” (9). Because paramagnetic structures had a higher resonance frequency, the phase of small veins was often negative and appeared dark relative to the brain parenchyma and CSF on the phase image. The phase mask was created by setting all positive phase values (between 0 and $+180^\circ$) to unity and by normalizing the negative phase values (from 0 to $-\pi$) to a gray scale of values ranging linearly from 1 to 0 (Fig 1). This normalized phase mask was multiplied against the original magnitude image and yielded images that maximized the negative intensities of the veins. A minimum intensity projection technique was used to display the processed data using contiguous sections of thickness from 3 to 10 mm in the axial plane.

Preliminary results were available for 10 patients. All of the cavernomas diagnosed using conventional MR imaging were visible on HRBV images (seven cases); not only were the margins of the lesions better defined but HRBV showed additional malformations compared with T2*-weighted images in two cases (Fig 2). Lesions that were presumed to be telangiectasias were shown on HRBV images (two cases); one showed non-specific contrast enhancement (Fig 3), and the other was invisible on conventional images (Fig 4). Numerous vessels were shown on HRBV images compared with the conventional contrast-enhanced images, but it was not possible to ascertain whether these vessels were part of the venous lesions or a concurrent telangiectasia (one case) (Fig 5).

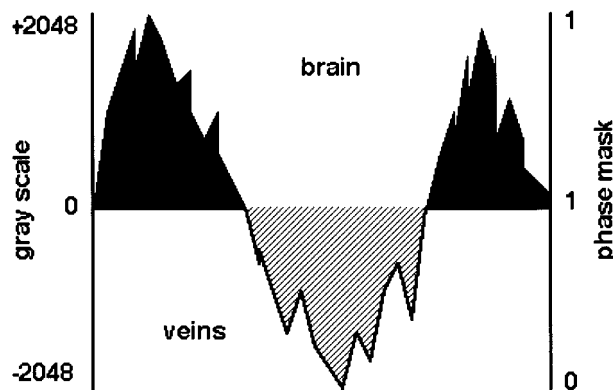


FIG 1. Diagram representative of the phase behavior of brain and veins. The phase mask is created by setting to unity (black regions) all positive phase values (0 to $+2048$), and negative phase values (0 to -2048) are displayed on a scale of 1 to 0 (hashed region).

Received November 6, 1998; accepted after revision, March 24, 1999.

From Washington University School of Medicine, St. Louis Children's Hospital, Mallinckrodt Institute of Radiology, St. Louis, MO.

Address reprint requests to Benjamin C.P. Lee, MD, Department of Radiology, St. Louis Children's Hospital, One Children's Place, St. Louis, MO.

FIG 2. Comparison of HRBV and T2*-weighted images.

A, T2*-weighted echo-planar image (TE, 40) shows the susceptibility effects of multiple cavernomas. Susceptibility is present in the right frontal region.

B, HRBV image shows numerous additional lesions. Note that the margins of the cavernomas are defined better with this technique.

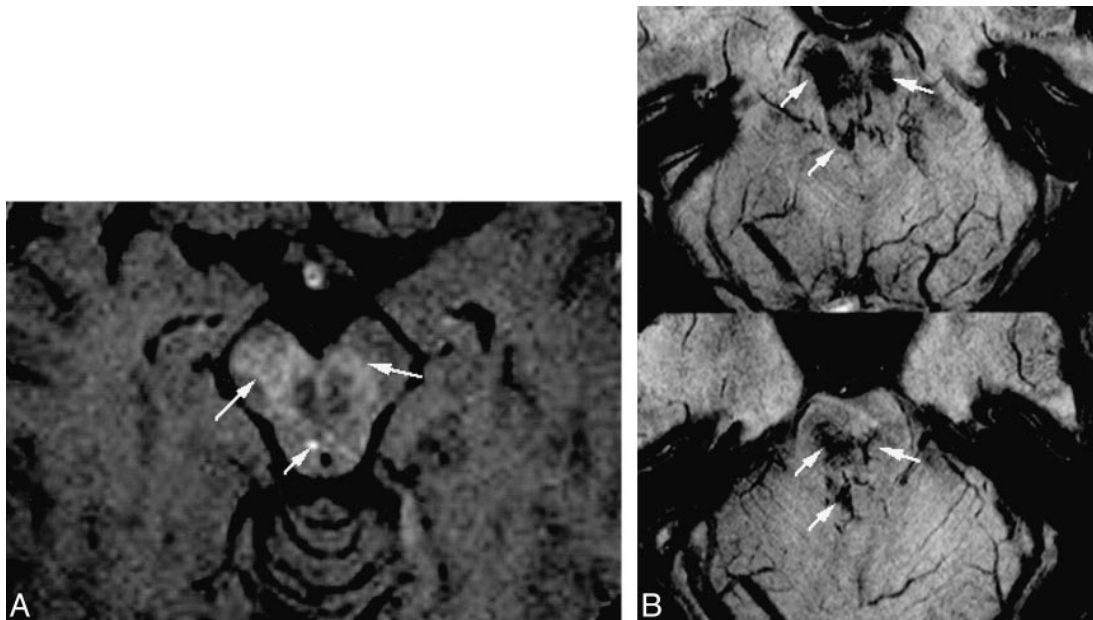
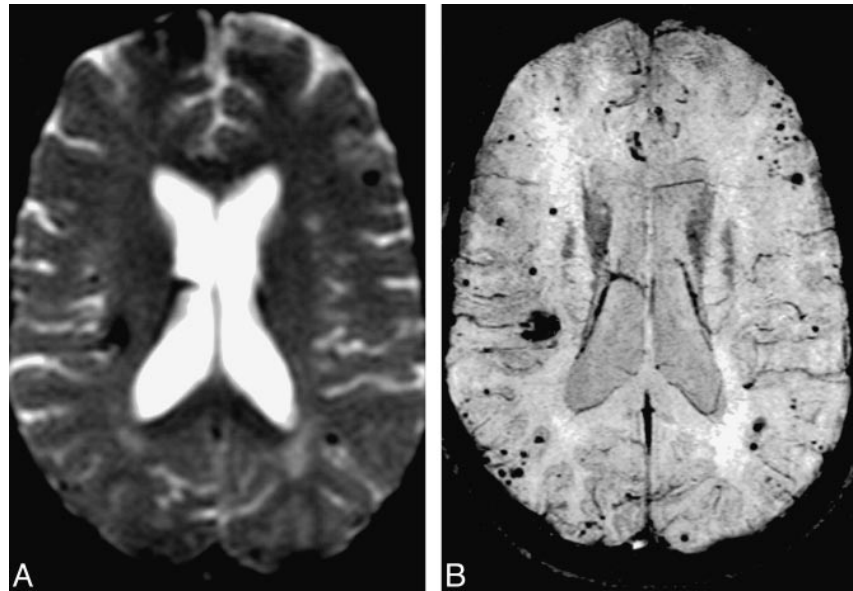


FIG 3. Comparison of HRBV and contrast-enhanced T1-weighted images.

A, Contrast-enhanced T1-weighted image (750/20 [TR/TE] with one acquisition) shows slight enhancement (arrows).

B, HRBV image shows abnormal vessels in the same regions compatible with telangiectasias. Some of the vessels have configurations of veins.

Discussion

Cavernomas are detectable on MR images by virtue of the signal of hemorrhage and flow void within the abnormal vessels. Contrast enhancement is inconstant and often nonspecific (1–6, 10). Time-of-flight and phase-contrast angiography rely on the presence of moving blood and are best in detecting vessels in the sensitized direction. These techniques are much less effective when the malformed vessels are organized in a multidirectional and complex manner. The slow flow within the vessels of the malformations poses additional difficulty

because of blood signal saturation. Large vessels within malformations are visible after contrast; small vessels are often not detected because of the partial volume effect of the relatively large voxel used in conventional imaging.

HRBV relies on the magnetic properties and the associated differences in relaxation rates between venous and arterial blood or brain issue. The difference in bulk volume susceptibility between oxygenated and deoxygenated red blood cells accounts for both phase changes and T2-weighted differences between arterial and venous blood. It is

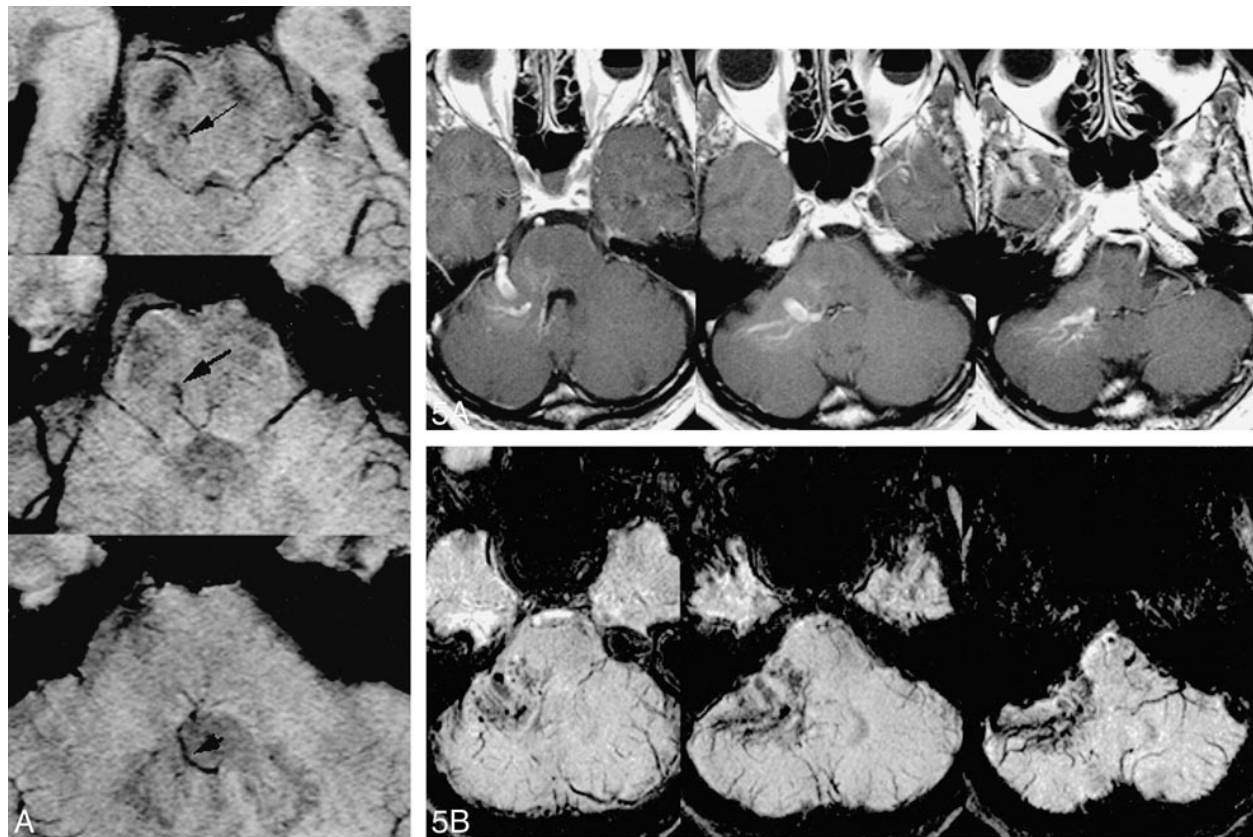


FIG 4. HRBV image shows a small vascular blush (arrow), which is a presumed telangiectasia, and an adjacent draining vein (arrowhead).

FIG 5. Comparison of HRBV and contrast-enhanced T1-weighted images.

A, Contrast-enhanced T1-weighted image (750/20 with one acquisition) shows enhancement of a typical venous angioma in the right cerebellopontine angle.

B, HRBV image shows numerous small vessels in addition to the enhancing vessels seen on the contrast study. These small vessels may represent small venous malformations or telangiectasias.

possible to differentiate deoxygenated from oxygenated blood by using the HRBV gradient-echo technique with appropriately long echo times. This technique exploits the signal losses in venous blood from both T2-weighted and phase changes. The bulk susceptibility shift effect of deoxygenated blood causes a frequency shift of the protons, which leads to a phase difference between venous blood and tissue spins. Because of the partial volume effect of venous blood with surrounding tissue, there is signal cancellation in the reconstructed magnitude images if the protons in the venous blood and brain tissue are out of phase. This phase reversal of venous blood causes a cancellation of signal from the brain parenchyma. For a signal fraction of blood of λ and for brain parenchyma of $1-\lambda$, the signal intensity changes in tissue mixed with venous blood reduces from 1 to $1-2\lambda$ in the opposed phase condition described above. This cancellation is the essence of the venous enhancement phenomenon used in this study (9). The unique feature of the technique is the phase mask used for data processing, which renders the HRBV exquisitely sensitive to small BOLD changes. When the magnitude images are multiplied by the phase mask, there is enhancement of the venous

data but no change in the magnitude signal where veins are not present. The resulting magnitude images are displayed, using the minimum intensity projection. This technique is the converse of the maximum intensity projection and displays low-signal differences of the veins, minimizing the high signals of the brain tissue (9).

Intracerebral veins of all sizes are visible routinely on HRBV because of the small voxel size. Vessels smaller than the voxel are detected with this technique by virtue of the susceptibility inherent in the BOLD effect, which causes signal loss beyond the immediate vicinity of the vessels (8). Although it might be possible to detect small vessels with conventional T2*-weighted echo-planar images, provided the voxel size is reduced, this technique does not have the benefit of the enhancing effect of the phase mask. We rely on the curvilinear configuration of the vessels on the minimum intensity projection to identify discrete veins, but we are currently unable to differentiate visually small patent vascular malformations from those that have thrombosed or bled. It is, however, possible to characterize patent vessels by a careful analysis of the phase pattern; for a patent venous vessel, the phase will fall within a well-known limit

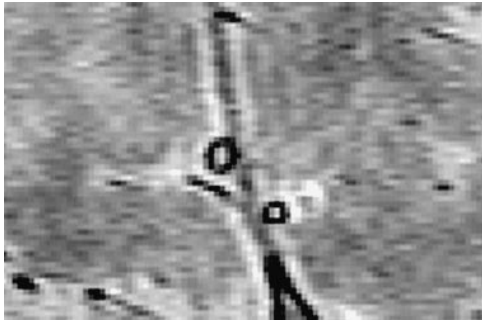


FIG 6. HRBV image shows an example of the "ring" effect of two veins.

based on an oxygen saturation of 55%. Pooled blood that has clotted is likely to have a much longer phase effect (expected to be four times higher) because of the increased hematocrit and reduced oxygen saturation compared with slowly flowing venous blood. For a moderately large vein, the lumen occupies several voxels and often will exhibit a phase close to π , so that it is nullified. The peripheral portion of the vessel will appear dark because of the partial volume effect (Fig 6).

HRBV is acquired using a modification of the 3D gradient-echo technique, which is available in most modern scanners. Postprocessing of the data takes approximately 20 minutes and is performed off-line using a program developed at this institution (8, 9). It is entirely feasible to incorporate this process into the reconstruction software of future scanners. This technique is ideal for screening patients with a high clinical suspicion of low-flow vascular malformations, such as cavernomas and telangiectasias. It is of less use in the diagnosis of venous malformations, because these are usually

visible on conventional scans. An important finding in our preliminary data is the ability of HRBV to reveal cavernomas that are invisible on T2*-weighted images. Sequential HRBV may be used to determine whether cavernomas that increase in number with time arise de novo or merely represent subsequent bleeding from previously unrecognized small malformations.

References

1. New PFJ, Ojeman RG, Davis KR, et al. **MR and CT of occult vascular malformations of the brain.** *AJNR Am J Neuroradiol* 1986;7:771-779
2. Rigamonti D, Drayer BP, Johnson PC, Hadley MN, Zabramski J, Spetzler RF. **The MRI appearance of cavernous malformations (angiomas).** *J Neurosurg* 1987;67:517-524
3. Barker CS. **Magnetic resonance imaging of intracranial cavernous angiomas. A report of 13 cases with pathological confirmation.** *Clin Radiol* 1993;48:117-121
4. Latchaw RE, Truwit CL, Heros RC. **Venous angioma, cavernous angioma, and hemorrhage.** *AJNR Am J Neuroradiol* 1994;15:1255-1257
5. Tomlinson FH, Houser OW, Scheithauer BW, Sundt TM, Okazaki H, Parisi JE. **Angiographically occult vascular malformations. A correlative study of features on magnetic resonance imaging and histological examination.** *Neurosurgery* 1994;34:792-797
6. Vogler R, Castillo M. **Dural cavernous angioma. MR features.** *AJNR Am J Neuroradiol* 1995;16:773-775
7. Marchal G, Bosmans H, Fraeyenhoven LV, Wilms G, Hecke PV, Plets C.A.L.B. **Intracranial vascular lesions. Optimization and clinical evaluation of three-dimensional time-of-flight MR angiography.** *Radiology* 1990;175:443-448
8. Reichenbach JR, Venkatesan R, Schillinger DJ, Kido DK, Haacke EM. **Small vessels in the human brain. MR venography with deoxyhemoglobin as an intrinsic contrast agent.** *Radiology* 1997;204:272-277
9. Reichenbach JR, Venkatesan R, Yablonsky DA, Thompson MR, Lai S, Haacke EM. **Theory and application of static field inhomogeneity effects in gradient-echo imaging.** *J Magn Reson Imaging* 1997;7:266-279
10. Atlas SW, Mark AS, Grossman RI, Gomori JM. **Intracranial hemorrhage. Gradient-echo MR imaging at 1.5 T. Comparison with spin-echo imaging and clinical applications.** *Radiology* 1988;168:803-807